Microstructure and Formation Process of the Characteristic Reddish Color Pattern Hidasuki on Bizen Stoneware: Reactions Involving Rice Straw

Yoshihiro Kusano,*,† Minoru Fukuhara,‡ Tatsuo Fujii,§ Jun Takada,§ Ryu Murakami,|| Akira Doi,† Laurence Anthony,+ Yasunori Ikeda,@ and Mikio Takano@

Department of Applied Arts and Design, Kurashiki University of Science and the Arts, 2640 Nishinoura, Tsurajima-cho, Kurashiki-shi, Okayama 712-8505, Japan, Department of Applied Chemistry and Department of Information and Computer Engineering, Okayama University of Science, 1-1 Ridai-cho, Okayama 700-0005, Japan, Department of Applied Chemistry, Okayama University, 3-1-1 Tsushima-naka, Okayama 700-8530, Japan, Nara National Cultural Properties Research Institute, 94-1 Miyanowaki, Kashihara 634-0025, Japan, and Institute for Chemical Research, Kyoto University, Uji, Kyoto-fu, 611-0011, Japan

Received November 24, 2003. Revised Manuscript Received July 19, 2004

The formation process of Hidasuki, a characteristic reddish coloring pattern on traditional Japanese unglazed stoneware called Bizen, was studied through model experiments. Pellets of the same type of clay used to form Bizen stoneware were heated to 1250 °C with and without contact with rice straw and then were cooled at different rates. A reddish color appeared for relatively slowly cooled samples when rice straw was present. Owing to the presence of potassium in the rice straw, the mullite ($3(Al,Fe)_2O_3 \cdot 2SiO_2$), the major phase formed in the absence of rice straw, was replaced by corundum (α-Al_2O_3), hematite (α-Fe_2O_3), and others in the surface region of about 50 μm in depth. The corundum precipitated as hexagonal platelike crystals, and on the edges of these crystals the hematite grew epitaxially. The growth continued so that the primary corundum crystals were wholly covered by hematite to form a specific single crystalline α-Fe_2O_3/α-Al_2O_3/α-Fe_2O_3 structure. The contribution of this unique microstructure to coloring is discussed. On the basis of these analytical results, the Hidasuki pattern was reproduced artificially in the form of written characters.

Introduction

Bizen stoneware, one example of artistic Japanese unglazed ceramics, has been loved for over 1000 years because people perceive wabi and sabi from this stoneware. Here, wabi is a concept of the richness and beauty in simplicity and poverty, and sabi is an aesthetic sense of existing loneliness. The art is considered to be an art of clay and flame because the different colors of red, orange, purple, yellow, black, silver, and gold appear in various forms without the aid of artificial glazing or dyeing figures. Fine control of these patterns is, however, extremely difficult because multiple parameters such as the chemical composition of the clay, firing temperature, cooling rate, and effective oxygen partial pressure are involved. We believe, however, that studies of the essential coloring mechanism from the viewpoint of solid-state chemistry can provide artists with new inspiration and chemists with new concepts with respect to the creation of novel functional materials.

In this study, we focus on Hidasuki, a characteristic reddish pattern appearing specifically where the clay contacts rice straw,[1] which is used primarily as a separator to prevent the adhesion of stoneware in the kiln. The reddish color is known to be derived from hematite. We note here that the clay mined from the Bizen area in Okayama prefecture, Japan contains approximately 2−3 wt % of Fe_2O_3[2] and also that rice straw generates SiO_2 (84 wt %) and K_2O (13 wt %) when heated at 1000 °C in air. As reported in our previous paper, a glassy phase forms through reactions of the clay with the potassium provided by rice straw in which small and red hematite crystals precipitate on cooling.[3] In this paper, we report the evolution of a specific microstructure through model experiments.

* To whom correspondence should be addressed. Tel. and fax: +81 86 440 1051. E-mail: yoshi-k@arts.kusa.ac.jp.
† Kurashiki University of Science and the Arts.
‡ Department of Applied Chemistry, Okayama University of Science.
§ Okayama University.
|| Nara National Cultural Properties Research Institute.
+ Department of Information and Computer Engineering, Okayama University of Science.
@ Kyoto University.

(1) Miyagawa, I. *Glaze*; Kyoritsu Shuppan Co., Ltd.: Tokyo, 1965; pp 84−85.
(2) Doi, A.; Sakamoto, N.; Tsutsumi, S.; Ohtsuka, R.; Kato, C. *J. Chem. Soc. Jpn. Chem. Industrial Chem.* **1979**, 71.
(3) Yamaguchi, K.; Kusano, Y.; Fukuhara, M.; Doi, A.; Takada, T. *J. Jpn. Soc. Powder Powder Metallurgy* **1992**, *39*, 79.

10.1021/cm0352145 CCC: $27.50
Published on Web 08/25/2004

Table 1. Chemical Composition of Clay Mined from Bizen Area[a]

SiO_2	Al_2O_3	Fe_2O_3	CaO	MgO	MnO	K_2O	P_2O_3
83.95	0.58	0.06	0.85	0.61	0.32	12.74	0.89

[a] Unit of numbers in the table is weight percent (wt %). Trace amounts of Ba (536 ppm), Cr (64), Cu (22), Ni (27), Pb (29), Rb (117), Sr (75), V (98), Y (37), Zn (87), Zr (167), F (239), Cl (116), and S (446) were included.

Table 2. Chemical Composition of Rice Straw Ash[a]

SiO_2	TiO_2	Al_2O_3	Fe_2O_3	CaO	MgO	MnO	K_2O	Na_2O	P_2O_5	Ig. loss
63.51	0.69	21.61	2.77	0.56	0.66	0.03	2.05	0.51	0.04	7.57

[a] Unit of numbers in the table is weight percent (wt %).

Experimental Procedures

The starting dried Bizen clay powder (less than 106 μm in diameter) contains quartz, halloysite, montmonrillonite, and feldspar as the main crystalline materials. The clay powder was pelleted to 20 mm in diameter and then heated with and without rice straw covering the surface at various temperatures up to 1250 °C in air or in mixed O_2/N_2 gases with various oxygen contents. This temperature is near to that in real kilns. The heating rate was 1 °C/min. The samples were then quenched or cooled to 800 °C at different rates of 1−10 °C/min and then to room temperature rapidly. The crystalline phases formed were identified through powder X-ray diffraction measurements on the as-prepared pellets (XRD, CuK_α radiation, Rigaku RINT2100). Microstructure observations were carried out with transmission electron microscopy (TEM, Topcon EM-002B equipped with energy-dispersive X-ray analyzer (EDS) and JEOL JEM-4000EX). The samples for TEM were prepared as follows. First, the surface of a sample pellet was treated with 1 M hydrofluoric acid for 5 min for the purpose of isolating crystalline phases from a glassy matrix. Then, the crystals were dispersed in carbon tetrachloride and collected on a copper grid with a perforated carbon-film support. The chemical compositions of the clay and ash rice straw heated at 1000 °C were analyzed with X-ray fluorescence spectroscopy (XFS, Rigaku RIX2100) as summarized in Tables 1 and 2, respectively. Mössbauer spectra were obtained at room temperature from the as-prepared sample surfaces using the backscattering technique. The ^{57}Co source was kept at room temperature, and the control sample for velocity calibration was metallic iron.

Results and Discussion

Figure 1 shows the colors of the sample pellets heated in air at 1250 °C with rice straw put on their surface. Sample R1250Q (Figure 1a) was quenched, while samples R800/10 (Figure 1b) and R800/1 (Figure 1c) were cooled from 1250 to 800 °C at a rate of 10 and 1 °C/min, respectively. Suggesting the importance of the cooling process, R1250Q is not reddish, but R800/10 and R800/1 are, and the color tone is deeper for the latter.

Sample NR800/1 heated in air at 1250 °C and cooled 800 °C at 1 °C/min without rice straw contains quartz (SiO_2), cristobalite (SiO_2), and mullite in its surface region as can be seen in Figure 2a. On the other hand, mullite was absent, but corundum and hematite appeared in its place when heated with rice straw as can be seen for R1250Q (Figure 2b). At the same time, the very broad reflection, owing to a glassy matrix, increased and shifted its peak position to lower *d*-spacing. These results suggest that the presence of rice straw suppressed the formation of mullite or induced a decomposition of mullite to corundum, hematite, and

Figure 1. Colors of samples heated with rice straw on the surface in air at 1250 °C and then (a) quenched (R1250Q), (b) cooled to 800 °C at a rate of 10 °C/min (R800/ 10), and (c) cooled to 800 °C at 1 °C/min (R800/1). The tone of the reddish color became deeper with decreasing cooling rate.

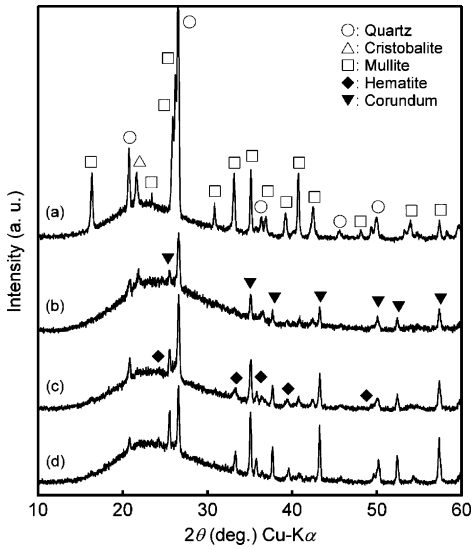

Figure 2. XRD patterns of (a) a sample heated without rice straw on the surface in air at 1250 °C and cooled at a rate of 1 °C/min (NR800/1). Panels b−d are for samples heated with rice straw on the surface in air at 1250 °C and then quenched (R1250Q) and cooled to 800 °C at a rate of 10 °C/min (R800/ 10) and 1 °C/min (R800/ 1), respectively.

amorphous phases. It should be noted here anyway that mullite can contain ferric ions up to approximately 10% in total, which substitute for aluminum sites.[4−17] The brownish color of NR800/1 is probably caused by the Fe^{3+}-containing mullite, $3(Al,Fe)_2O_3{\cdot}2SiO_2$.[14]

For the reddish samples R800/10 (Figure 2c) and R800/1 (Figure 2d), the reflections from corundum and

(4) Brownell, W. E. *J. Am. Ceram. Soc.* **1958**, *41*, 226.
(5) Murthy, M. K.; Hummel, F. A. *J. Am. Ceram. Soc.* **1960**, *43*, 267.
(6) Schneider, H.; Rager, H. *J. Am. Ceram. Soc.* **1984**, *67*, C-248.
(7) Ménil, F. *J. Phys. Chem. Solids* **1985**, *46*, 763.
(8) Schneider, H.; Rager, H. *Ceram. Int.* **1986**, *12*, 117.
(9) Schneider, H. *J. Am. Ceram. Soc.* **1987**, *70*, C-43.
(10) Cardile, C. M.; Brown, I. W. M.; Mackenzie, K. J. D. *J. Mater. Sci. Lett.* **1987**, *6*, 357.
(11) Parmentier, J.; Vilminot, S.; Dormann, J. L. *Solid State Sci.* **1999**, *5*, 257.
(12) Ocaña, M.; Caballero, A.; González-Carreño, T.; Serna, C. *J. Mater. Res. Bull.* **2000**, *35*, 775.
(13) Djemai, A.; Balan, E.; Morin, G.; Hernandez, G.; Labbe, J. C.; Muller, J. P. *J. Am. Ceram. Soc.* **2001**, *84*, 1017.
(14) Djemai, A.; Calas, G.; Muller, J. P. *J. Am. Ceram. Soc.* **2001**, *84*, 1627.
(15) Ronchetti, S.; Piana, M.; Delmastro, A.; Salis, M.; Mazza, D. *J. Euro. Ceram. Soc.* **2001**, *21*, 2509.
(16) Soro, N.; Aldon, L.; Fourcade, J. O.; Jumas, J. C.; Laval, J. P.; Blanchart, P. *J. Am. Ceram. Soc.* **2003**, *86*, 129.
(17) Kusano, Y.; Doi, A.; Nakanishi, M.; Fujii, T.; Takada, J.; Fukuhara, M.; Murakami, R. *Proceedings of Science for New Technology of Silicate Ceramics*; Techna Srl: Faenza, 2003; p 39.

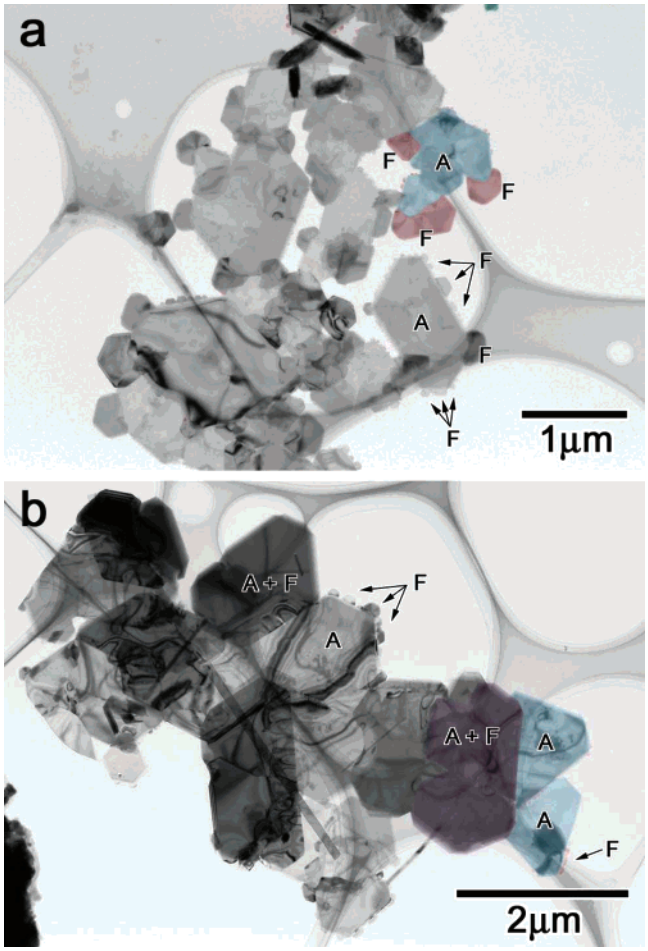

Figure 3. TEM images for samples (a) R800/10 and (b) R800/1. In panel a, large platelike particles that are blue and/or marked A are corundum, and small relatively dark ones surrounding the corundum crystals, some of which are red and/or marked F, are hematite. In panel b, relatively light particles, some of which are blue and/or marked A, are corundum with tiny hematite crystals on the edges attached, while the dark ones, some of which are purple and/or marked A + F, are corundum particles wholly covered by hematite like α-Fe_2O_3/α-Al_2O_3/α-Fe_2O_3.

hematite were enhanced, suggesting that these oxides increased in amount and grew in size during slow cooling. Another remarkable observation is that the relative abundance of corundum to hematite increased as the cooling rate was decreased (compare Figure 2c,d), suggesting that the formation of corundum occurred during the slow cooling and that hematite slowly followed the formation of corundum. TEM results to be shown next provided us with a vivid image of what occurred in the cooling process.

The crystalline phases obtained from samples R800/10 and R800/1 are shown in Figure 3a,b, respectively. According to EDS and electron diffraction (ED) measurements, the relatively large platelike particles seen in Figure 3a, some of which are blue and marked A for the sake of easy identification, are corundum, while the smaller and darker platelike particles, some of which are red and marked F, are hematite. It is known that corundum and hematite form aluminum- and iron-rich solid solutions of $Al_{2-x}Fe_xO_3$ with approximately $x <$ 0.28 and >1.9 at 1250 °C and that the solubility decreases at lower temperature for both.[18] Hereafter, we call these corundum and hematite, respectively, for simplicity. In Figure 3b, the hematite appears to have grown in size because almost all the particles are morphologically similar to each other. The EDS examination indicated, however, that iron was concentrated in the relatively dark particles such as the one that is purple and marked A + F. We will come back to this point later.

We note here that all the corundum crystals observed were platelike. This oxide usually assumes a hexagonal rodlike shape but can form a hexagonal platelike shape when synthesized in the presence of additional elements such as Si, Ca, Mg, and Na,[19−22] which are all contained in the present clay.

Summarized in Figure 4 are TEM images for the sample R800/10, which reveal a close relation between corundum and hematite. In Figure 4a, a corundum crystal of approximately 1.5 μm in width is covered by hematite crystals of about 0.5 μm or less in width. Note that both pure corundum ($x = 0$) and hematite ($x = 2$) crystallize in the same structure of $R\bar{3}c$ with $a = 0.4758$ nm and $c = 1.2991$ nm (JCPDS No.10-0173) and $a = 0.5036$ nm and $c = 1.3749$ nm (JCPDS No.33-0664) in hexagonal setting, respectively. The ED patterns of hexagonal symmetry shown in the inset indicate that the growth proceeded preferentially in their basal planes. Moreover, the crystal directions are the same throughout this ensemble, indicating an epitaxial relation between these phases. There is one exceptional hematite crystal that seems to have grown on the flat surface of the mother crystal, but in fact, a close examination revealed that the growth occurred at a step edge, not on the flat surface directly. The hematite overgrowth appears to take place on the plate edges of corundum.

In Figure 4b, it is possible to observe that five hematite crystals are going to completely cover a small corundum crystal. This view is supported by the cross sectional [$\bar{1}2\bar{1}0$] TEM image in Figure 4c where a thin corundum crystal is found embedded in a thick hematite crystal. Thus, the relatively large and dark particles such as the ones that are purple and/or marked A + F in Figure 3b are corundum crystals wholly covered with hematite. Here and also in Figure 4a,b, moiré patterns with a fringe spacing of approximately 4.4 nm can be seen in the regions where hematite overlaps with corundum. The fringe spacing is in good agreement with the value of 4.3 nm calculated from the in-plane lattice constants of these crystals. The appearance of the moiré patterns is additional evidence for the epitaxial relationship. To our best knowledge, a microstructure consisting of two single crystalline structures, one sandwiching the other, has not been reported.

Here, we will discuss the formation of corundum. For simplicity, we assume that the present clay is the K−Al−Si−O system containing K_2O, Al_2O_3, and SiO_2 at a ratio 3.1:24.6:72.3 in wt %. For this composition

(18) Levin, E. M.; Robbins, C. R.; McMurdie, H. F. *Phase Diagrams for Ceramists*; The American Ceramic Society: Columbus, OH, 1964; Vol.1, Figure 27, p 43.
(19) Song, H.; Coble, R. L. *J. Am. Ceram. Soc.* **1990**, *73*, 2077.
(20) Song, H.; Coble, R. L. *J. Am. Ceram. Soc.* **1990**, *73*, 2086.
(21) Goswami, A. P.; Roy, S.; Mitra, M. K.; Das, G. C. *J. Am. Ceram. Soc.* **2001**, *84*, 1620.
(22) Jin, X.; Gao, L. *J. Am. Ceram. Soc.* **2004**, *87*, 533.

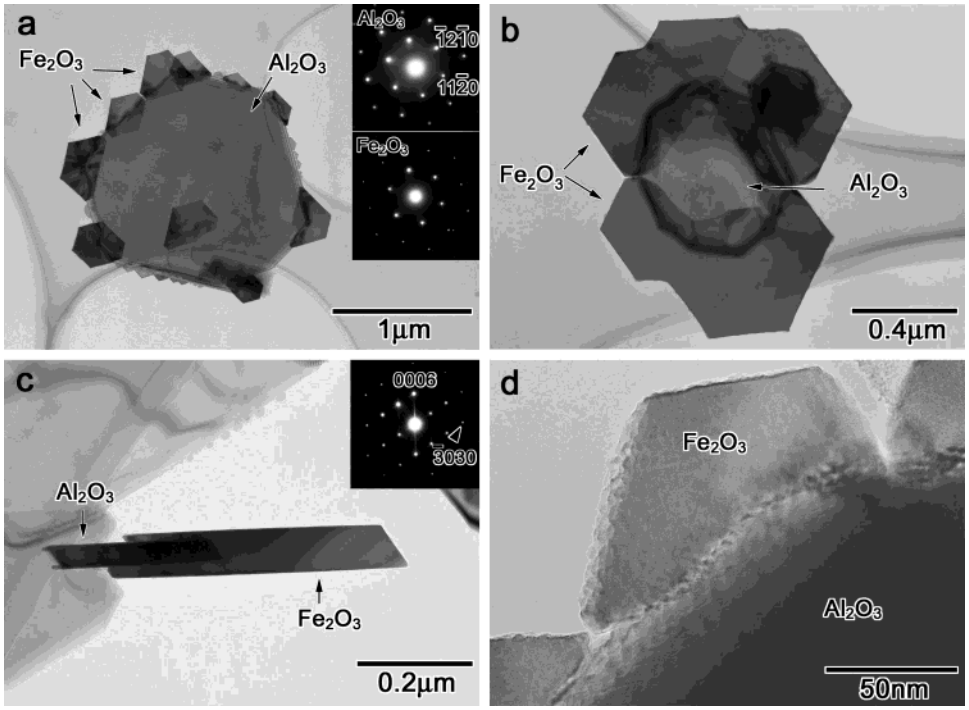

Figure 4. TEM images and ED patterns for sample R800/10. The images shown in panels a and b were the [0001] zone axis of corundum and hematite, respectively. Hematite epitaxially grew on the edges of corundum particles. (c) Cross-sectional [$\bar{1}2\bar{1}0$] TEM image showing a part of the α-Fe_2O_3/α-Al_2O_3/α-Fe_2O_3 sandwich-like structure. Shown in panel d is the boundary region between a hematite crystal and a corundum edge.

heated in air at 1200 °C, three phases exist, including a liquid phase, SiO_2, and mullite,[23] but corundum is absent. Pure mullite is very stable,[24] but the addition of iron and potassium suppresses the formation of mullite or induces decomposition of mullite once formed in the heating process to corundum plus a liquid phase as found in our previous work in which a mixture of pure mullite, hematite, and potassium chloride was heated to 1250 °C in air.[25] In the present case, rice straw increased the K^+ content locally, while Fe^{3+} came from the clay itself. This rice straw-aided precipitation of platelike corundum crystals followed by the epitaxial growth of hematite is almost certainly the key to the formation of the Hidasuki pattern.

Figure 5 shows the Mössbauer spectra of samples NR800/1 (a) and R800/1 (b). A magnetic component assignable to hematite[26] was clearly observed in addition to a paramagnetic component for R800/1 (b), whereas only a paramagnetic component was observed for sample NR800/1 (a). The absence and the presence of hematite in NR800/1 and R800/1 is consistent with the XRD results. The isomer shift (IS) and the quadrupole splitting (QS) of the paramagnetic component are IS = 0.357 mm/s and QS = 1.11 mm/s for NR800/1 and IS = 0.329 mm/s and QS = 0.56 mm/s for R800/1. Generally speaking, the parameters for NR800/1 are consistent with those for Fe^{3+} dissolved in mullite, but as is well-known, both tetrahedral and octahedral sites

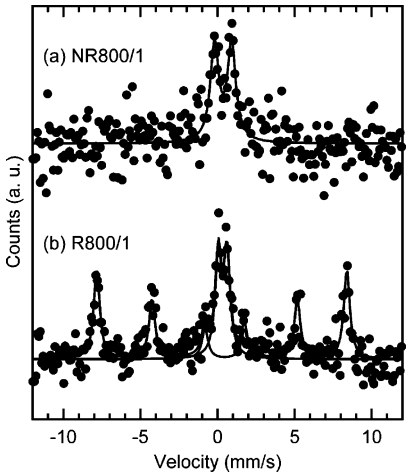

Figure 5. Mössbauer spectra of the pellet surfaces of NR800/1 (a) and R800/1 (b).

are available for iron dissolved in mullite.[6−16] Because the low iron content of the clay we used made the signal-to-noise ratio of the spectrum poor, we could not say more than that the spectrum of NR800/1 came from the ferric ions incorporated in the mullite structure.

According to Ménil's classification, the IS values for Fe^{3+} ions at tetrahedral and octahedral sites are confirmed in the ranges of 0.1−0.30 and 0.28−0.50 mm/s, respectively.[7] The IS (= 0.329 mm/s) for the paramagnetic component of R800/1 is on the borderline. The relatively small QS value of the paramagnetic component of this sample indicates that these ferric ions are not any more dissolved in mullite. However, whether these are dissolved in corundum or in the glassy phase remains uncertain.

Next, we briefly describe the influence of oxygen partial pressure during the heat treatment on the phase

(23) Levin, E. M.; Robbins, C. R.; McMurdie, H. F. *Phase Diagrams for Ceramists*, 4th ed.; The American Ceramic Society: Columbus, OH, 1979; Figure 407, p 156.
(24) Aksay, I. A.; Pask, J. A. *J. Am. Ceram. Soc.* **1975**, *58*, 507.
(25) Yamaguchi, K.; Kusano, Y.; Fukuhara, M.; Doi, A. *J. Chem. Soc. Jpn., Chem. Industrial Chem.* **1991**, 1073.
(26) Murad, E.; Johnston, J. H. *Mössbauer Spectroscopy Applied to Inorganic Chemistry, Vol. 2*; Plenum Publishing Corporation: New York, 1987; pp 507−582.

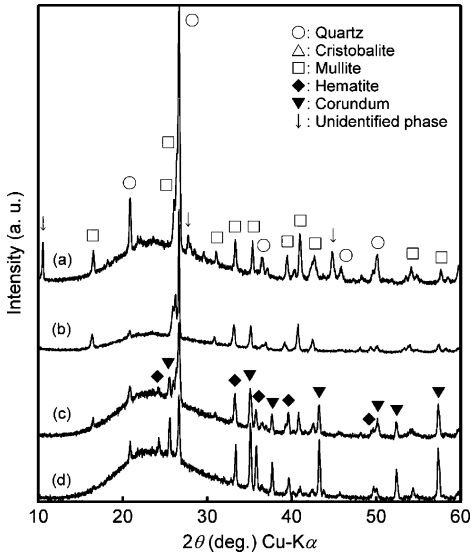

Figure 6. XRD patterns of the samples heated at 1250 °C and then cooled to 800 °C at a rate of 1 °C/min in N_2/O_2 = 100:0 (vol %) (a), 99:1 (b), 98:2 (c), and 95:5 (d).

formation. Figure 6 shows the XRD patterns of the samples treated in the same way as R800/1 but in mixed gases of N_2/O_2 = 100:0 (a), 99:1 (b), 98:2 (c), and 95:5 (d) in vol %. The sample for Figure 6a did not contain corundum or hematite, and the sample surface was black. On the other hand, the samples heated in the gases with oxygen of 2% or more (b−d) were reddish and contained both corundum and hematite. Hidasuki needs oxygen of 2% or more in the kiln. Three phases, mullite, corundum, and hematite, coexisted in the sample in panel c, while in the sample in panel d with the deepest reddish color tone on the surface, mullite disappeared, and the XRD intensities of corundum and hematite became maximum.

In this paragraph, we will discuss the very initial stage in the formation of the specific structure found previously. One scenario assumes that corundum first precipitates and that ferric ions, migrating through amorphous regions, are anchored on the edges. The *c*-plane surface of a corundum crystal is very smooth, but the edges, or the growth front, are reactive with kinks and steps (see Figure 4d). Probably, these sites provide the hematite with nucleation sites, and the hematite crystals contain dislocations caused by the lattice misfit as can be seen in Figure 4d, typically. The other scenario assumes that iron-containing corundum is formed initially, from which iron ion is expelled on cooling because the solubility is decreased. The reason that the hematite is deposited at the edges of the primary particles may be understood considering the structural features. The corundum structure is made of a hexagonal close-packed oxygen sublattice with only two-thirds of the octahedral voids being filled with cations. The vacancies should provide the ferric iron with linked diffusion paths. Then, one might ask why there are hematite-free corundum crystals in Figure 3b, but in fact, all the corundum crystals have some hematite attached.

We judge the former to be the case because the lattice constants of corundum remain the same within experimental error for Figures 2b−d. The lattice constants

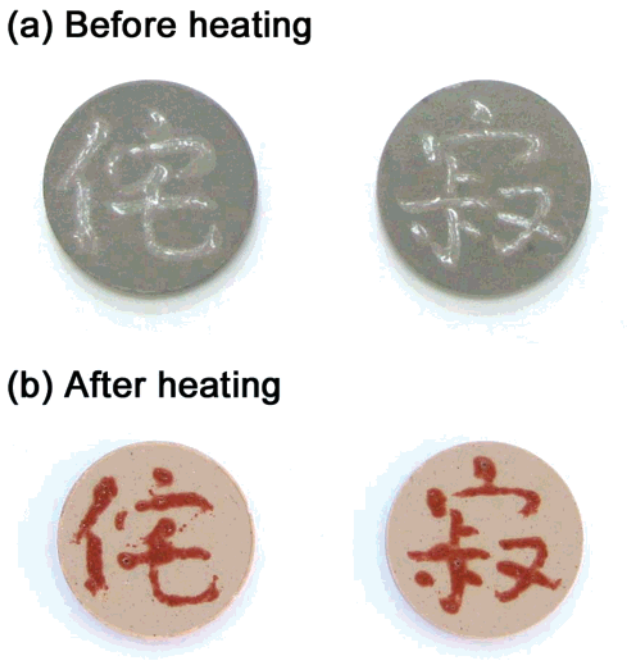

Figure 7. Hidasuki pattern artificially drawn in the form of Chinese characters, wabi (left) and sabi (right).

should have decreased gradually if iron was contained initially and the content decreased in the cooling process. Thus, the specific structure such as seen in Figure 3b seems to result from the following three sequential steps, which are the precipitation of pure, iron-free corundum particles, the anchoring of iron dissolved in the liquid phase at the edges of the corundum particles, and the subsequent epitaxial growth of hematite leading to the formation of nearly single crystalline particles with a unique α-Fe_2O_3/α-Al_2O_3/α-Fe_2O_3 sandwich structure.

Here occurs a favorable situation for coloring because an undesirably wide distribution in the size of the hematite particles is suppressed when the corundum crystals are rather uniform in size as experimentally observed. It is known that hematite particles seen with the eye change their color from vermilion (fine particles) to black (large particles). The hematite particles do not aggregate or stack; thus, the color tone is preserved. Moreover, the specific single crystal-like α-Fe_2O_3 on α-Al_2O_3 structure is believed to result in the clarity of the reddish color of hematite. However, owing to the low density of hematite in the surface region and also to the thinness of the layer (∼50 μm), the yellowish color of the mullite-rich region under the surface is not shielded completely, and these regions thus function in harmony.

On the basis of these results, we artificially drew the Hidasuki pattern in the form of Chinese characters as shown in Figure 7. On the surface of clay pellets, the characters were handwritten with a brush soaked in ethyl alcohol with potassium chloride dispersed homogeneously (a), and the pellets were heated to 1250 °C at 1 °C/min in air and then cooled to 800 °C at 1 °C/min (b). The characters are wabi (left) and sabi (right). This success should open up a way to artificially controlled patterning soon.

Conclusions

The coloring mechanism of the reddish Hidasuki pattern was studied from the viewpoint of solid-state chemistry through model experiments. The formation of a specific, nearly single crystalline α-Fe_2O_3 on α-Al_2O_3 composite structure is the key to the coloring. Rice straw contributed to the realization of this unusual microstructure by providing potassium. In this sense, it is interesting to note that potassium chloride and other alkali-containing salts also yield similar results. The usefulness of potassium chloride can be seen in Figure 7. We note here that KNO_3, KBr, and KI are also effective for the formation of Hidasuki, although the glass formation temperature is quite different. We believe that many interesting solid-state chemistries remain hidden in traditional technologies.

Acknowledgment. The authors are indebted to Prof. M. Ausloos (Université de Liège), Prof. R. Cloots (Université de Liège), and Dr. P. B. Vandiver (Smithsonian) for helpful discussions. This study was partly supported by a Grant-in-Aid for Scientific Research on the Priority Area by the Ministry of Education, Culture, Sports, Science and Technology of Japan, No. 14023115, 2002.

Note Added after ASAP Posting. The cross-sectional designation for the TEM image in Figure 4c was incorrect and other minor typographical errors were found in the version posted ASAP on August 25, 2004. The web version posted September 14, 2004 and the print version are correct.

CM0352145